



# Topography modeling of laser polishing on AISI 316L milled surfaces

Benoit Rosa, Jean-Yves Hascoët, Pascal Mognol

## ► To cite this version:

Benoit Rosa, Jean-Yves Hascoët, Pascal Mognol. Topography modeling of laser polishing on AISI 316L milled surfaces. *Mechanics & Industry*, 2014, pp.51-61. 10.1051/meca/2014003 . hal-01149683

**HAL Id: hal-01149683**

**<https://hal.science/hal-01149683>**

Submitted on 13 May 2015

**HAL** is a multi-disciplinary open access archive for the deposit and dissemination of scientific research documents, whether they are published or not. The documents may come from teaching and research institutions in France or abroad, or from public or private research centers.

L'archive ouverte pluridisciplinaire **HAL**, est destinée au dépôt et à la diffusion de documents scientifiques de niveau recherche, publiés ou non, émanant des établissements d'enseignement et de recherche français ou étrangers, des laboratoires publics ou privés.

# Topography modeling of laser polishing on AISI 316L milled surfaces

BENOIT ROSA<sup>a</sup>, JEAN-YVES HASCOËT AND PASCAL MOGNOL

Institut de Recherche en Communications et Cybernétique de Nantes (IRCCyN), UMR CNRS 6597, Nantes, France

Received 13 September 2013, Accepted 8 January 2014

**Abstract** – Laser polishing is a finishing process based on melting material, with the objective of improving surface topography. Some operating parameters must be taken into consideration, such as laser power, feed rate, offset, and overlap. Moreover, because of its dependence on the primary process, the initial topography has also an impact on the final result. This study describes a quadratic model, conceived to optimize final topography according to the primary process and laser polishing. Based on an experimental matrix, the model takes into account both laser operating parameters and the initial topography, in order to predict polished surfaces and to determine an optimal set of parameters. Furthermore, uncertainties linked to the measuring device need to be taken into consideration, as well as the process variability, in order to facilitate the interpretation of the results. After the phase of experimentation and the creation of the quadratic model, an optimal final topography is introduced, taking into account the initial surface and the laser parameters. Finally, in order to reduce the time process, it is important to study the impact of laser polishing strategy on the surface roughness.

**Key words:** Laser polishing / initial topography / experimental design / variability of process / quadratic model

## 1 Introduction

Finishing operations on mechanical parts is a decisive step in the production chain, regarding the functionality of parts. In the molding field, the finishing process is often practiced manually, which represents up to 30% of production cost [1]. These high costs are the result of high time processing operations that represent 10 to 30 min.cm<sup>-2</sup> and require highly qualified operators [1,2]. Moreover, the geometrical shape of parts can be modified by un-mastered trajectories and efforts applied to the surface. The accessibility of a complex shape is also restricting [2]. Then, from a health point of view, operators are exposed to the risk of inhaling metal powders. They are also exposed to musculo-skeletal pathologies caused by repetitive task movements. The economical context forces the industrial companies to reduce production costs by automating the processes. In order to improve surface quality and to reduce processing time, some finishing processes were developed such as the six axis mechanical polishing robot. However, the accessibility of complex surfaces is limited by the abrasive diameter

of tools. To improve the accessibility of complex surfaces laser polishing technology appears as notably promising.

Used a few years ago to polish diamonds [3,4] or optical lenses [5], the laser polishing technique is now chosen more frequently, especially to polish metals, thereby decreasing processing time and reaching 10 to 200 s.cm<sup>-2</sup> according to the initial topography.

The energy of the laser beam is applied to the surface and the topography peaks are melted. With the surfaces tensions, the molten material flow is reallocated into cavities in order to smooth the initial topography (Fig. 1).

The final topography depends on the operating parameters of the laser on the material, and is also linked to the initial topography and the strategy of laser polishing [6,7].

### 1.1 Problematic

Few studies are focused on the optimization of laser polishing surfaces according to the primary process in context of large and complexes shapes, such as mold surfaces [8–10]. In this context, and to create a multi-processes optimization [11], this study introduces a statistical model of prediction. The surface quality optimization is realized according to primary process and laser

<sup>a</sup> Corresponding author:  
[Benoit.Rosa@irccyn.ec-nantes.fr](mailto:Benoit.Rosa@irccyn.ec-nantes.fr)

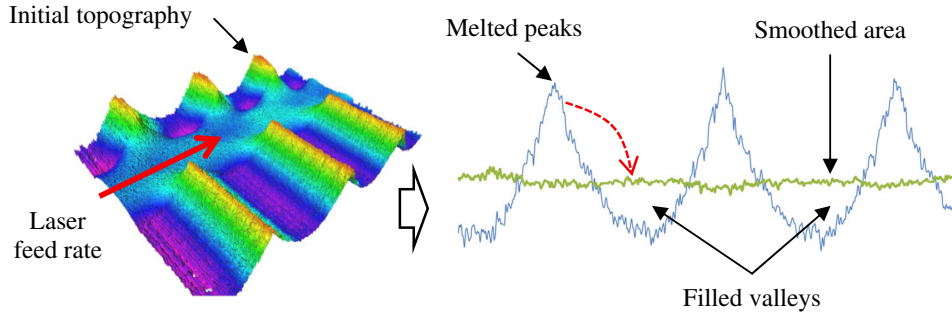


Fig. 1. Principle of laser polishing.

polishing in order to decrease the processing time of the whole manufacturing chain. As a result, this study introduces a coupled optimization between the primary process and the laser polishing. The model includes the initial topography, realized with a hemispherical tool, operating parameters of laser and the overlap parameter. The following parameters are used to control the laser:

- Laser power ( $P$ ) [W].
- Feed rate of the laser ( $V_f$ ) [mm.min<sup>-1</sup>].
- Offset ( $O_f$ ) [mm] which is the shift into laser's focal point and surface.
- Overlap ( $O_v$ ) [%] which means the distance a line overlaps with the last one. This parameter is specific for the treatment of a complete surface.

The milled surfaces obtained with a hemispherical tool are characterized by scallop height ( $H_c$ ) (Fig. 2), which is a function of the radius of hemispheric milling tool  $R$  and the milling step ( $a_e$ ) (Eq. (1)).

$$H_c = \frac{a_e^2}{8R} \quad (1)$$

The final surface is characterized by two parameters:

- Surface roughness parameter  $S_a$ , which is the arithmetic average heights of the surface [12] (Eq. (2)).
- Percent reduction of surface roughness. This parameter gives information about surface roughness reduction, using the initial surface roughness [7] (Eq. (3)).

$$S_a = \frac{1}{A} \iint_A |z(x, y)| dx dy \quad (2)$$

Surface roughness reduction (%) =

$$\frac{S_{a_{\text{initial}}} - S_{a_{\text{polished}}}}{S_{a_{\text{initial}}}} \times 100 \quad (3)$$

Different initial topographies were studied through the parameter  $H_c$ , in order to decrease the time of the primary process, and optimizing at the same time the reduction percentage of the initial surface roughness according to both processes.

The present paper focuses on the modeling and coupled optimization of laser polishing on AISI 316L milled surfaces. The modeling is taking into account the initial topography and the laser operating parameters.

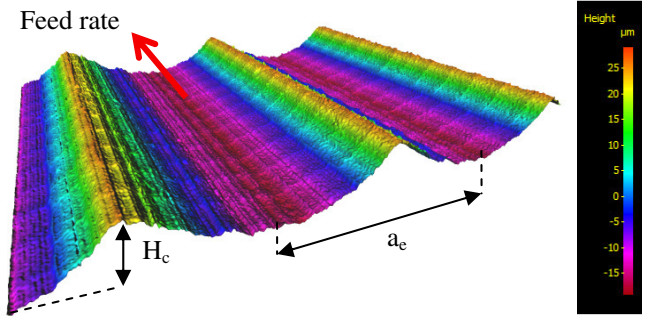


Fig. 2. Characteristics parameters of milled surface, measured by focal variation microscopy.

To facilitate a future industrial application, the methodology of investigation allows the establishment of a prediction/optimization protocol. Thanks to this protocol, the technique could be used by a final user. After the experimental study and the building of the modeling, an optimal surface can be presented. Finally, in order to improve the understanding of results and to optimize time process of laser polishing, uncertainties of measure have been analyzed and a study of polishing strategy is then presented.

## 1.2 Proposal for a protocol

In order to forecast the final topography and to determine an optimal set of parameters, an experimental approach was adopted. This experimental study includes the initial milled topography, the laser parameters and the overlap parameter. The aim of this protocol (Fig. 3) is to predict a final surface topography. The quality of the final surface is optimized, and so are the processing times of primary and laser polishing. The validity of the mathematical model depends on the experimental domain. The final user can choose the input parameters in order to predict the required roughness of polished surface. Therefore, the final topography and the processes time can be adjusted with the input parameters.

## 2 Experimental study

### 2.1 Laser type

A continuous fiber laser was used during the experimentation. The maximum laser power is 12 kW for a

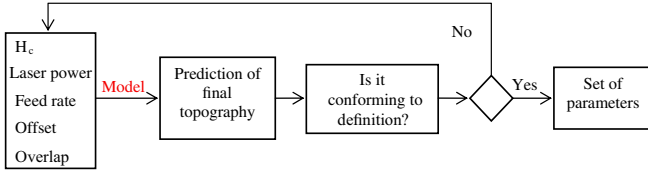


Fig. 3. Protocol.

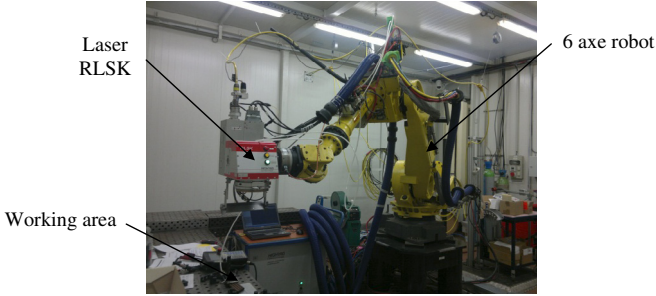


Fig. 4. Test experiment material.



Fig. 5. Operating principle of focal variation microscope.

600  $\mu\text{m}$  fiber's diameter. A welding head High Yag RLSK SWS was positioned on a six axes robot so as to carry-out the experiments (Fig. 4). The welding head allows the motion of the laser beam independently of the robot. To protect surfaces from oxidation, argon gas was employed during the laser polishing process.

## 2.2 Material of measure

The measurements were carried-out thanks to a focal variation microscope ALICONA Infinite focus (Fig. 5). This equipment allows for the obtention of a three-dimensional topography of polished surfaces. The roughness parameters are extracted after a 3D-reconstruction established through the software used.

## 2.3 Uncertainties of measure and variability of process

The expanded uncertainty ( $U$ ) equation (4) is obtained by multiplying the combined standard uncertainty ( $u_c$ ) by a coverage factor ( $k$ ). In this study, the

Table 1. Uncertainty of repeatability.

Parameter	$U_{\text{repeatability}}$	Unit
$S_a$	0.002	$\mu\text{m}$

Table 2. Uncertainty of area of measure.

Parameter	$U_{\text{area of measure}}$	Unit
$S_a$	0.017	$\mu\text{m}$

Table 3. Uncertainty of variability of process.

Parameter	$U_{\text{variability}}$	Unit
$S_a$	0.096	$\mu\text{m}$

coverage factor is chosen with a level of confidence of 99% ( $k = 3$ ). The standard uncertainty ( $u_c$ ) is obtained by equation (5).

$$U = u_c k \quad (4)$$

$$u_c = \frac{\sqrt{\frac{\sum (x_i - \bar{x})^2}{n-1}}}{\sqrt{n}} \quad (5)$$

### 2.3.1 Uncertainty of repeatability

The calculation of repeatability was performed on ten tests with exactly the same settings:

- luminosity;
- contrast;
- dimensions and location of the studied area.

According to the test results, the uncertainty of repeatability was negligible on the surface roughness parameter ( $S_a$ ) (Tab. 1).

### 2.3.2 Uncertainty of studied area

To calculate the surface parameters, an area needs to be selected. This selection is arbitrary, and its impact on the results needs to be known. Different areas were chosen in order to calculate the uncertainty of this parameter. The second result shows that the uncertainty of the area of measure is insignificant (Tab. 2) on the surface roughness parameter.

### 2.3.3 Process variability

The variability process was performed on eight polished surfaces with exactly the same laser parameters and the same initial topography. As shown in Table 3, the variability of the laser polishing process has an impact on the surface roughness parameter. According to the results, the surface roughness parameter is bounded by an uncertainty interval of  $\pm 0.1 \mu\text{m}$ .

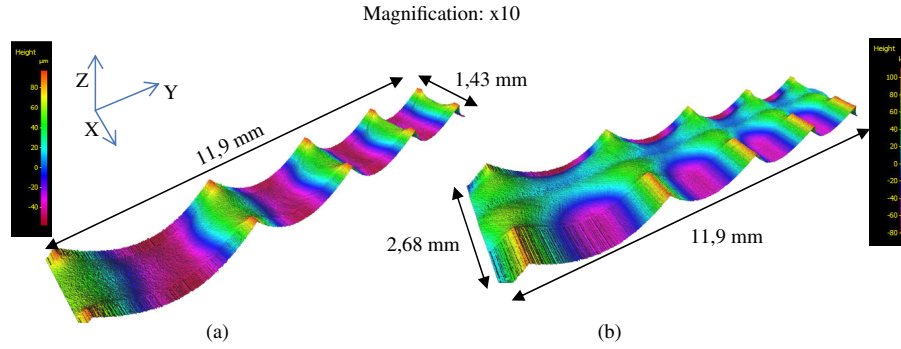


**Fig. 6.** Final topographies for scallop height of  $150\ \mu\text{m}$  and for laser powers of 600 W (a) and 1300 W (b).

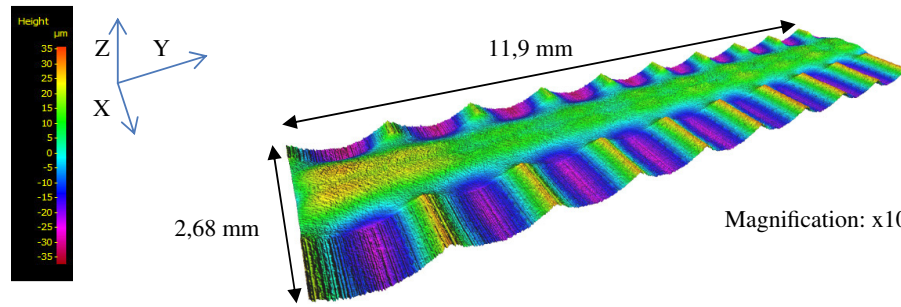


**Fig. 7.** Final topography for scallop height of  $50\ \mu\text{m}$  and laser power of 950 W.

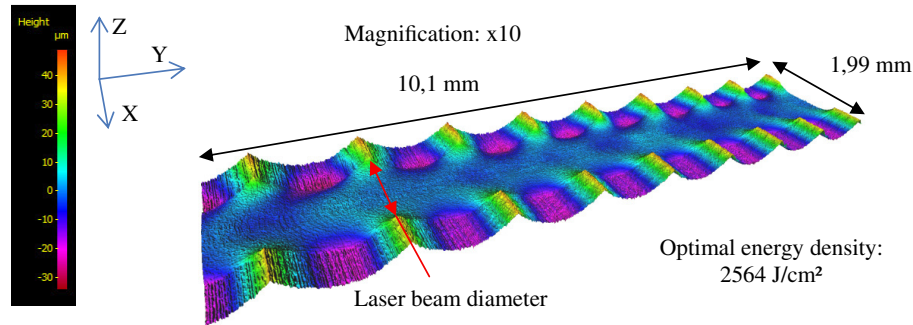


**Fig. 8.** Optimal final topography ( $H_c = 60\ \mu\text{m}$ ,  $P = 750\ \text{W}$ ,  $V_f = 1500\ \text{mm}\cdot\text{min}^{-1}$  and  $O_f = 30\ \text{mm}$ ).

## 2.4 Line polishing tests

This step was performed following a full experimental design divided into 27 tests. The laser parameters were based on the bibliography (Tab. 4) [1, 10]. The input parameters were: the scallop height, the laser power, the feed rate and the offset. In order to simplify this first experimental step, the polished tests were performed on polished lines. In that event, the overlap parameter that enables to polish surfaces was not used. The polished lines were perpendicular to the initial topography.

This first experimental step focused on the study of parameters that were judged the most influent, such as scallop height and laser power. The measured topographies showed that the scallop height of  $150\ \mu\text{m}$  was more important. Indeed, the laser power of 600 W (Fig. 6a) did not totally melt the peaks of the initial topography. On the contrary, for a power of 1300 W the topography was degraded (Fig. 6b).

**Table 4.** Parameters of full experimental design.

Factors	Levels		
Laser power [W]	600	950	1300
Feed rate [ $\text{mm}\cdot\text{min}^{-1}$ ]	1500	1700	1900
Offset [mm]	0	10	20
Scallop height [ $\mu\text{m}$ ]	50	150	

Concerning the scallop height of  $50\ \mu\text{m}$ , a setting of 950 W improved the smoothing result (Fig. 7). However, the smoothing is not optimal and parameters need to be adjusted.

This first step of the experiment showed that the initial topography has an impact on the final one. Indeed, there is an optimal scallop height. After this first step of experiments, the input parameters were adjusted and an optimal topography was obtained (Figs. 8 and 9).



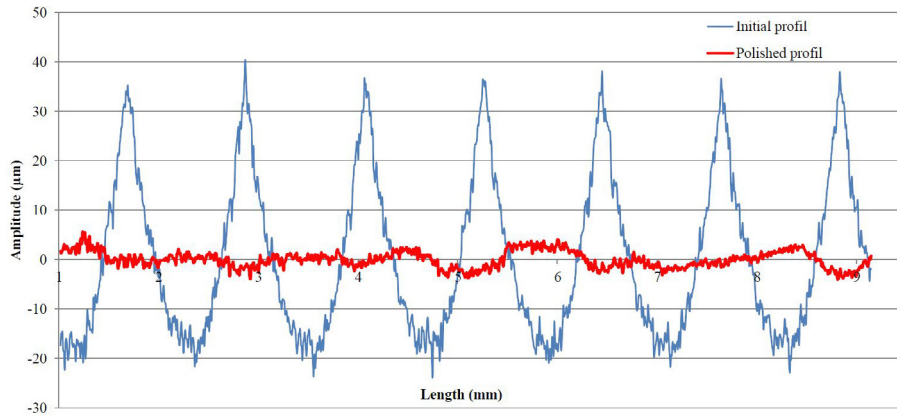


**Fig. 9.** Optimal topography profile on  $Y$  axis ( $H_c = 60 \mu\text{m}$ ;  $P = 750 \text{ W}$ ;  $V_f = 1500 \text{ mm}\cdot\text{min}^{-1}$ ;  $O_f = 30 \text{ mm}$ ).

**Table 5.** Experimental design of Taguchi  $L_{16}^{(4,5)}$ .

Trial	$H_c$	Laser power	Feed rate	Offset	Overlap
	$\mu\text{m}$	W	$\text{mm}\cdot\text{min}^{-1}$	mm	%
1	40	750	500	0	20
2	40	850	1000	10	30
3	40	950	1500	20	40
4	40	1050	2000	30	50
5	50	750	1000	20	50
6	50	850	500	30	40
7	50	950	2000	0	30
8	50	1050	1500	10	20
9	60	750	1500	30	30
10	60	850	2000	20	20
11	60	950	500	10	50
12	60	1050	1000	0	40
13	70	750	2000	10	40
14	70	850	1500	0	50
15	70	950	1000	30	20
16	70	1050	500	20	30

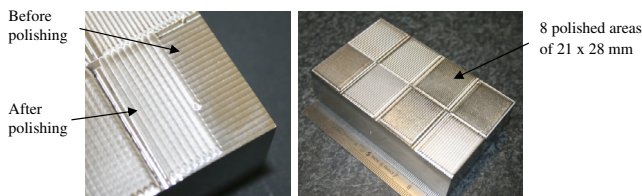


**Fig. 10.** Design of samples.

## 2.5 Surface polishing tests

This second step was performed according to an experimental design based on  $L_{16}^{(4,5)}$  Taguchi method (Tab. 5). This design experiment contains 5 factors and 4 levels. The strategy of surface polishing was perpendicular to the initial topography and the input factors were: the scallop height, the laser power, the feed rate, the offset and the overlap parameter. In order to establish the percentage of overlap, the diameter of the laser beam must be measured. This step consists in measuring the real beams diameters for each energy density. This is applied to the

surface with a focal variation microscope in order to master the overlap parameter.

This experimental study was based on the first results, obtained with the first design experiment. For this purpose, the parameters of the second design experiment were adjusted. The advantages of the Taguchi design are the optimization of the number of trials. Indeed, to study the homogeneity of surfaces,  $21 \text{ mm} \times 28 \text{ mm}$  surfaces were employed (Fig. 10). Two samples AISI 316L were used, and were divided in 8 areas of  $21 \text{ mm} \times 28 \text{ mm}$ , each area corresponding to one test of the design experiment.

Choosing this type of design matrix (Tab. 5) was justified by the number of factors and by the number of levels. In this matrix, it is possible to integrate every factor of the problematic, such as: the characterization factor of the initial topography ( $H_c$ ), the laser power, the feed rate, the offset and the overlap. Fewer tests are necessary, and that could have an important effect on industrial application. A number of levels superior to two enable the approach of nonlinear systems. The optimal results of this experimental study (Tab. 6) are a surface roughness reduction of 85% and a final surface roughness of  $2.08 \pm 0.1 \mu\text{m}$

With  $P$  [W],  $V_f$  [mm/min] and  $\phi$  [mm].

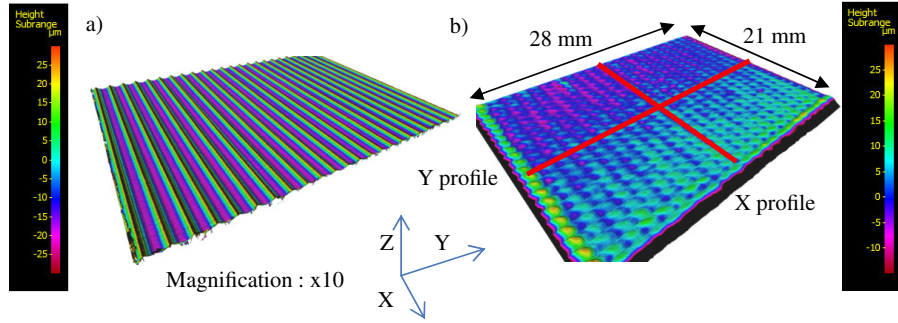


**Fig. 11.** Initial topography (a) and final topography (b) with optimal parameters ( $P = 750$  W;  $V_f = 1500$  mm.min<sup>-1</sup>;  $O_f = 30$  mm,  $H_c = 60$  μm and  $O_v = 30\%$ ).

**Table 6.** Experimental design and results.

Tests	$H_c$	Laser Power	Feed rate	Offset	Overlap	Laser beam diameter	$S_a$	$S_a$ reduction
	μm	W	mm.min <sup>-1</sup>	mm	%	mm	μm	%
1	40	750	500	0	20	1.73	4.5	54
2	40	850	1000	10	30	1.59	3.3	66
3	40	950	1500	20	40	1.46	4.8	51
4	40	1050	2000	30	50	1.35	5.2	47
5	50	750	1000	20	50	1.40	2.3	81
6	50	850	500	30	40	1.85	2.5	78
7	50	950	2000	0	30	1.57	6.3	46
8	50	1050	1500	10	20	1.59	4.4	63
9	60	750	1500	30	30	1.17	2.1	85
10	60	850	2000	20	20	1.30	3.9	72
11	60	950	500	10	50	1.78	3.3	76
12	60	1050	1000	0	40	1.77	5.2	62
13	70	750	2000	10	40	1.31	4.7	70
14	70	850	1500	0	50	1.59	6.1	62
15	70	950	1000	30	20	1.66	2.9	81
16	70	1050	500	20	30	1.94	7.6	52

for an initial surface roughness of  $13.73$  μm. The average surface roughness reduction of the overall trials is 65%.

A  $2500$  μm cut off filter was applied according to standard ISO 4288 in order to obtain correct surface roughness parameters. The dimensions of measured surfaces were  $17 \times 22$  mm. The optimal density of energy of the experiments is  $2564$  J.cm<sup>-2</sup>. The density of energy depends on three laser parameters: the laser power, the feed rate and the offset [10] (Eq. (6)). The efficiency of laser polishing has been highlighted by the smoothing of profile before polishing, and the decrease of the amplitude (Figs. 11 and 12).

$$E \left( \frac{\text{J}}{\text{cm}^2} \right) = \frac{6000 P}{\phi V_f} \quad (6)$$

with  $P$  [W],  $V_f$  [mm.min<sup>-1</sup>] and  $\phi$  [mm].

### 2.5.1 Impact of initial topography

The objective of this step is to study the impact of the initial topography onto the final topography. To carry this out, the average effects of laser power and scallop height on surface roughness are studied and compared. From the experimental test, it was possible to classify the input factors by its impact degree on the surface roughness. However, the experimental design was saturated. The saturation of experimental design means that the number of experiments is equal to the number of degrees of freedom. This saturation was caused by the affection of the factors on all columns of the experimental matrix. In this case, this experimental design was not helpful in the calculation of the interaction between the different factors. However, a logical analysis could be applied to the associated linear graph (Fig. 13). This linear graph indicates the positions of the interaction in the experimental design. The

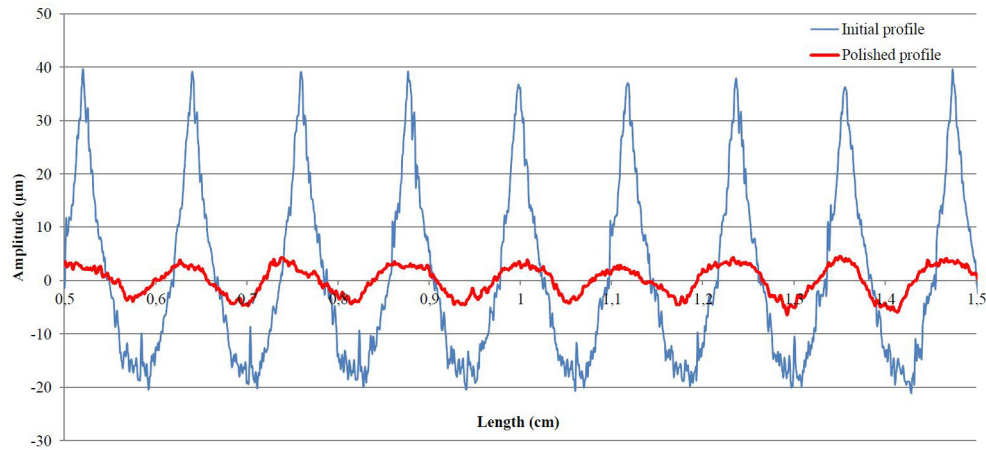


Fig. 12. Optimal topography profile of the experimental design on  $Y$  axis (85% of surface roughness reduction).

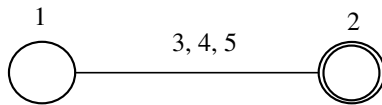


Fig. 13. Linear graph of the design experiment.

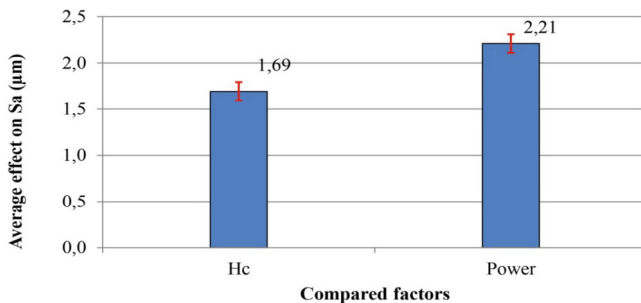


Fig. 14. Impact of initial topography on final surface roughness.

interaction between the scallop height and the laser power is located in the columns of the feed rate, the offset and the overlap.

Finally it is possible to compare the effects of the initial topography and the laser power on surface roughness because there is no interaction into both effects. The histogram (Fig. 14) shows a small difference between the effects of  $H_c$  and laser power on the surface roughness. To conclude, the initial surface is an important parameter, as well as the laser operating parameters, like laser power.

## 2.6 Optimization of final surface

The surface response method was employed in order to optimize the final surface topography according to the initial topography and the laser parameters. Based on quadratic regression between the experimental data and the input parameters, it is possible to determinate the optimum position of the reduction of the surface roughness. The surface responses showed that the optimal domain of

feed rate and  $H_c$  is in the experimental domain (Fig. 15a). For the laser power and  $H_c$  the optimal domain is also in the experimental domain (Fig. 15b). Finally, regarding the overlap parameter the optimal domain is not in the experimental domain (Fig. 15c). This observation shows a superior value of 50% improved surface roughness reduction. Moreover, the surface responses showed that a scallop height of 60  $\mu\text{m}$  is an optimal value according to the laser parameters.

The next step consisted in studying the increase of the overlap parameters for 60% and 90% of the values. These overlap values were applied with an optimal laser parameter determined from surfaces responses ( $H_c$  of 60  $\mu\text{m}$ , power of 750 W, 1000  $\text{mm}\cdot\text{min}^{-1}$  for the feed rate and 30 mm for the offset). According to these values of input parameters, the maximum surface reduction was 93%. According to the standard ISO 4288 a filter with a cut off of 800  $\mu\text{m}$  was used. The final  $S_a$  was  $0.94 \mu\text{m} \pm 0.1 \mu\text{m}$  (Fig. 16) for an initial  $S_a$  of 13.6  $\mu\text{m}$ . The augmentation of overlap considerably increased the final result.

After this optimization, the initial topography was eliminated. This optimal surface smoothing was highlighted by the decrease of the profile amplitudes and the decrease of frequency on the  $Y$  (Fig. 17) and  $X$  axes (Fig. 18).

The increase of the overlap parameter to 90% eliminated the initial topography without the increase of energy density. However, this observation was limited and the line polished tests showed it. Overall, the increase of overlap limits the impact of the initial topography but the  $H_c$  has an optimal value that depends on the energy density.

## 2.7 Impact of laser polishing strategy

In order to optimize processing time, the impact of the laser polishing strategy on the surface roughness has been studied through two different types of strategies. Both were perpendicular to the initial topography. The first was the Oneway strategy and the second one was



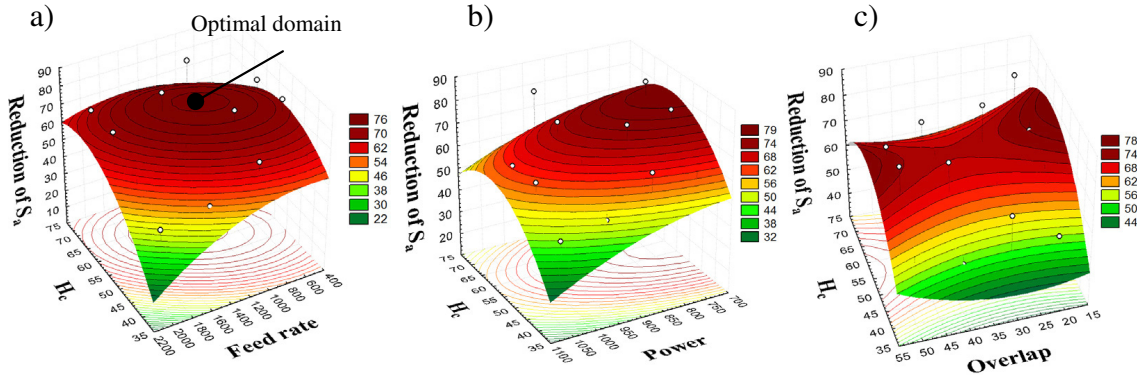


Fig. 15. Quadratic response surfaces between input parameters and the surface roughness reduction.

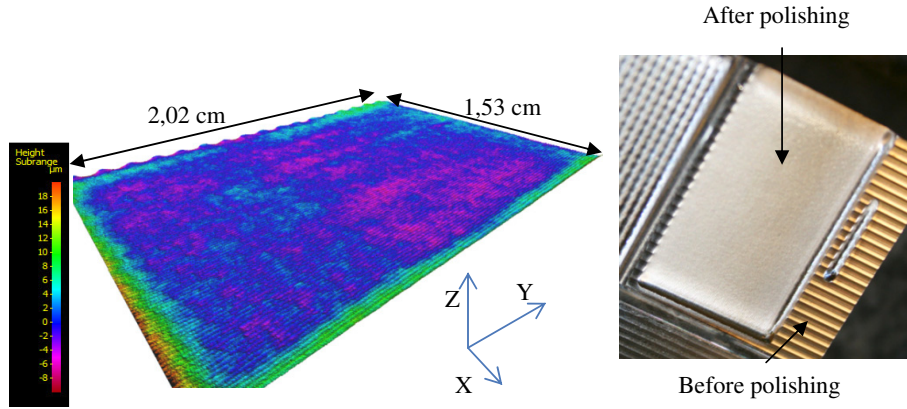


Fig. 16. Final topography for 90% overlap ( $H_c = 60 \mu\text{m}$ ,  $P = 750 \text{ W}$ ,  $V_f = 1000 \text{ mm} \cdot \text{min}^{-1}$  and offset = 30 mm).

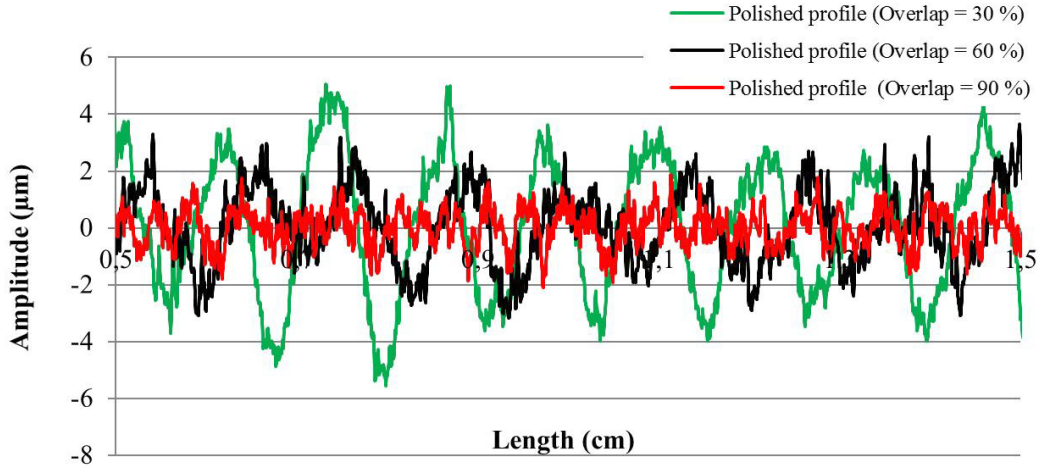


Fig. 17. Topography profiles for different overlap parameters on Y axis (Overlap 30, 60 and 90%).

the ZIG ZAG strategy (Fig. 19). In this study the initial topography and the laser parameters were the same for both the strategies.

The result (Tab. 7) shows how negligible the impact of the laser polishing strategy was on the surface roughness. The final surface roughness was the same for both strategies. To summarize, in order to decrease the processing time of laser polishing, the ZIG ZAG strategy seems to be more interesting.

### 3 Modeling

Current multi-physics models concentrate on small laser polished surfaces or laser polished lines. These multi-physics models need an important number of calculus, consequently they take up a lot of time which is not appropriate for the treatment of large industrial surfaces, such as mold surfaces. In molds industrial manufacturing context, the decrease of time calculus is important.

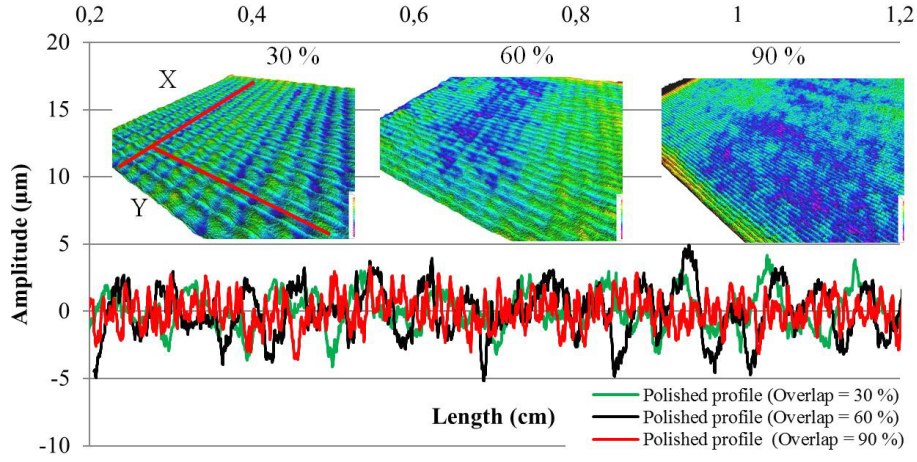


**Fig. 18.** Topography profiles for different overlap parameters on  $X$  axis and associated topographies (overlap 30, 60 and 90%).

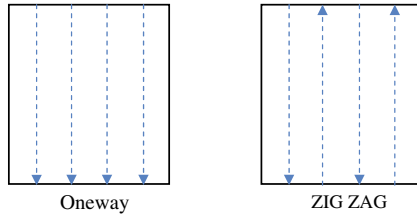


**Fig. 19.** Laser polishing strategies.

**Table 7.** Impact of the laser polishing strategy on the surface roughness parameter

	Oneway	ZIG ZAG
$S_a$ ( $\mu\text{m}$ )	2.03	2.05

In this context, a statistical model is used. Based on the Taguchi design (Tab. 6), this model functions for this experimental domain. As well as a nonlinear system [10], and a number of levels superior to 2, a quadratic model was used equation (7).

$$y_{\text{mod}} = b_0 + b_1x_1 + b_2x_2 + \dots + b_kx_k + b_{11}x_1^2 + b_{22}x_2^2 + \dots + b_{kk}x_k^2 \quad (7)$$

The input parameters are represented by  $x_1 \dots x_k$  and the coefficients (monomials) by  $b_0 \dots b_{kk}$ . The quadratic regression equation is divided into two parts: a linear part and a quadratic part expressed by squared factors. The number of monomials is a function of the number of factors and the number of degrees of regression. After having calculated the coefficients, the quadratic regression model was obtained equation (8).

$$\begin{aligned} \text{Roughness reduction of } S_a(\%) = & -166.77768 + 5.44880583H_c - 0.04559046H_c^2 \\ & + 0.221260766 \times \text{Power} - 0.1514 \cdot 10^{-3} \times \text{Power}^2 \\ & + 0.026068521 \times \text{Feed rate} - 0.12484 \cdot 10^{-4} \times \text{Feed rate}^2 \\ & + 0.643237507 \times \text{Offset} - 0.00642640 \times \text{Offset}^2 \\ & - 0.9232599 \times \text{Overlap} + 0.012452807 \times \text{Overlap}^2 \quad (8) \end{aligned}$$

The  $R^2$  parameters quantify the adjustment of model with the experimental results (Fig. 20).

The model is adjusted at 88% with the measured experimental values. But the adjustment is not perfect since the angle of the linear regression is different to  $45^\circ$ . The average percentage difference between the measured values and predicted value is 3.68%, for a maximum of 8.1% and a minimum of 0%.

## 4 Discussion of results

In order to test the predictive capacity of the model, the “leave one out” cross validation method was used. The aim of this methodology is to predict the extracted points of architecture of the model. In other words, this method relates the behavior of the model between the points used for statistical regression. Thus, a model is calculated for each point. Each model is based on  $N-1$  points and allows the prediction of the extracted point. After calculation of the 16 points, the average error of the model is 11.5% (Fig. 21). However, three predicted points have excessive errors. The maximum predicted error is 40% for a minimal error of 0.02%.

In order to test the real predictive capacity of this statistical model, a validation test was carried-out during the experimental campaign ( $H_c = 60 \mu\text{m}$ ;  $P = 750 \text{ W}$ ;  $V_f = 1000 \text{ mm} \cdot \text{min}^{-1}$ ;  $O_f = 30 \text{ mm}$  and  $O_v = 30\%$ ). The predicted value of the validation test is 87.38% and the measured value is 84.5%, the predicted error being 2.88%.

## 5 Conclusions and perspectives for further research

This study focuses on the topography modeling of laser polishing of AISI 316L milled surfaces. Experimental tests on laser polished lines allow the determination of optimal scallop height according to the laser polishing parameters. The second experimental campaign takes into

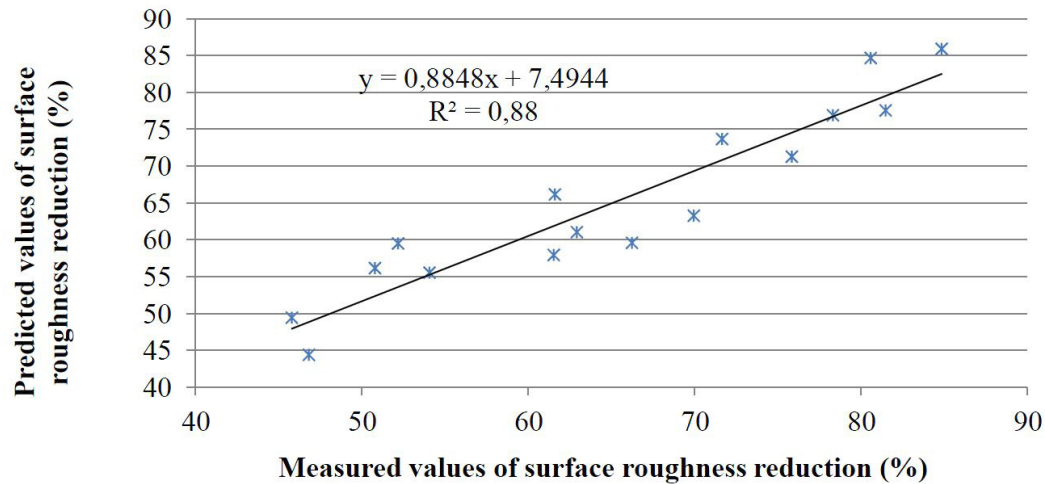


Fig. 20. Correlation of measured values and predicted values.

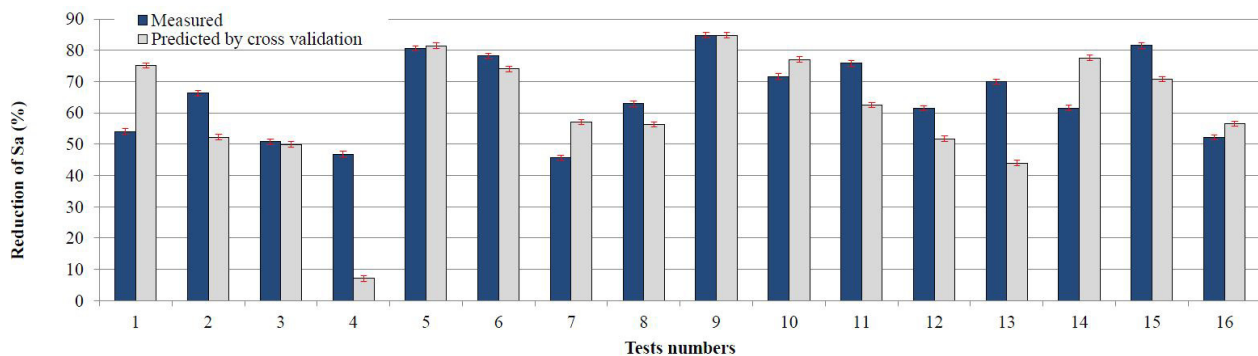


Fig. 21. Measured and predicted values by cross validation methodology.

consideration the initial topography, the laser parameters, the overlap parameter and allows for the creation of the statistical model. The protocol facilitates the optimization of the manufacturing processing time of the primary process and/or the laser polishing process. Having built the model facilitates the prediction of final surface roughness parameters. Indeed, the methodology of investigation takes into consideration the uncertainties of measure. According to these results, more conclusions can be established:

- The laser polishing process is effective with regard to surface smoothing. The laser parameters and the initial topography dispose of optimal values.
- The initial topography has an impact on the final topography. The initial surface is an important parameter, as well as the laser operating parameters such as laser power.
- The quadratic regression model based on experimental design of Taguchi  $L_{16}^{4,5}$  is adjusted to 88% of experimental values.
- Thanks to the “leave one out” cross validation method the predictive capacity of the model is acceptable. The average error is 11.5%.
- The surface responses are a good indicator with regard to the position of the optimum.

- The use of experimental matrix enables the obtention of an average percentage of roughness reduction of 65% for a maximum of 85%.
- The variability of the laser polishing process is acceptable and must be taken into consideration.
- After optimization, the percentage of surface roughness reduction is 93%, for a final surface roughness of  $0.94 \mu\text{m} \pm 0.1 \mu\text{m}$  and an initial surface roughness of  $13.6 \mu\text{m}$ .
- The laser polishing strategy does not impact the final surface roughness.

Further research will be focused on multi-scan strategy in order to increase the final quality of macro-polished surfaces. Furthermore, the research will concentrate on the laser polishing of thin section parts obtained by additive manufacturing. This context of study highlights the very high temperature involved in the laser polishing process which deeply changes the shape of the surface itself. In addition, it points out the characterization problem of the chaotic initial topography.

*Acknowledgements.* This work is co-funded by the European Union. Europe invests in Brittany with Regional Development European Funds (FEDER). The authors would like to thanks the Ecole Normale Supérieure de Rennes, the Technical Resource Centre of Morlaix and more particularly L.Dubourg from the Institute of Maupertuis.

## References

- [1] E. Ukar, A. Lamikiz, L.N. López de Lacalle, F. Liebana, J.M. Etayo, D. del Pozo, Laser Polishing Operation for Die and Moulds Finishing, *Adv. Mater. Res.* 83–86 (2009) 818–825
- [2] C. Nüsser, I. Wehrmann, E. Willenborg, Influence of Intensity Distribution and Pulse Duration on Laser Micro Polishing, *Physics Procedia* 12 (2011) 462–471
- [3] A. Erdemir, M. Halter, G.R. Fenske, A. Krauss, D.M. Gruen, S.M. Pimenov, V.I. Konov, Durability and tribological performance of smooth diamond films produced by Ar-C60 microwave plasmas and by laser polishing, *Surf. Coat. Technol.* 94–95 (1997) 537–542
- [4] S.Gloor, W. Lüthy, H.P. Weber, S.M. Pimenov, V.G. Ralchenko, V.I. Konov, A.V. Khomich, UV laser polishing of thick diamond films for IR windows, *Appl. Surf. Sci.* 138–139 (1999) 135–139
- [5] O.Y. Bol'shepaev, N.N. Katomin, laser polishing of glass articles, *Glass and Ceramics* 54 (1997) 141–142
- [6] E. Willenborg, Polishing with Laser Radiation, *Kunststoffe International* 97 (2007) 37–39
- [7] A.M.K. Hafiz, E.V. Bordatchev, R.O. Tutunea-Fatan, Influence of overlap between the laser beam tracks on surface quality in laser polishing of AISI H13 tool steel, *J. Manuf. Process.* 14 (2012) 425–434
- [8] A. Gisario, A. Boschetto, F. Veniali, Surface transformation of AISI 304 stainless steel by high power diode laser, *Opt. Lasers Eng.* 49 (2011) 41–51
- [9] A. Lamikiz, J. Sanchez, L. Lopezdelacalle, J. Arana, Laser polishing of parts built up by selective laser sintering, *Inter. J. Machine Tools Manuf.* 47 (2007) 2040–2050
- [10] E. Ukar, A. Lamikiz, L.N. López de Lacalle, D. del Pozo, J.L. Arana, Laser polishing of tool steel with CO2 laser and high-power diode laser, *Int. J. Machine Tools Manuf.* 50 (2010) 115–125
- [11] M. Rauch, R. Laguionie, J.Y. Hascoet, S.H. Suh, An advanced STEP-NC controller for intelligent machining processes, *Robotics and Computer-Integrated Manufacturing* 28 (2012) 375–384
- [12] Standard ISO 25178-2, Surface texture: areal. Parts 2: terms, definitions and surface texture parameters, 2012